

CHARGINO MASS AND R_b ANOMALY. *

Piotr H. Chankowski

Institute of Theoretical Physics, Warsaw University
 ul. Hoża 69, 00–681 Warsaw, Poland.

Stefan Pokorski †

Max–Planck–Institute für Physik
 Werner – Heisenberg – Institute
 Föhringer Ring 6, 80805 Munich, Germany

August 8, 2018

Abstract

We re-examine the possible magnitude of the supersymmetric contribution to R_b with imposed all available phenomenological constraints and demanding good quality of the global fit to the precision electroweak data. For low $\tan\beta$ we find a new region of the parameter space, with $M_2 \approx |\mu|$ and $\mu < 0$ where R_b remains large, ~ 0.2180 even for the lighter chargino as heavy as $90 - 100$ GeV. It is an interesting mixture of the up-higgsino and gaugino. The rôle of various phenomenological constraints is discussed in analytic form and importance of small but non-negligible left-right mixing in the stop sector is emphasized in this context. The large $\tan\beta$ option for enhancement of R_b is also reviewed. The available data do not rule out this scenario.

*Supported in part by the Polish Committee for Scientific Research and European Union Under contract CHRX-CT92-0004.

†On leave of absence from Institute of Theoretical Physics, Warsaw University

1. INTRODUCTION.

A considerable excitement has recently been inspired by the R_b and R_c anomaly [1, 2, 3, 4, 5, 6, 7, 8, 9]. The successful tests of the Standard Model (SM), to a per mille level [10], are challenged by the measurements of the partial widths of the Z^0 decays into $\bar{b}b$ and $\bar{c}c$ quarks which disagree with the SM predictions for $m_t = 180(170)$ GeV at the level of 3.7(3.5) and 2.5(2.5) standard deviations, respectively [11]. If both results are confirmed, the SM and its simplest supersymmetric extension, the Minimal Supersymmetric Standard Model (MSSM), are ruled out. However, since the R_b anomaly is statistically more significant, it is also of interest to discuss the possibility of explaining only the larger than in the SM value of R_b . Even if R_c is fixed to its SM prediction, $R_c = 0.172$ the then measured value of $R_b = 0.2206 \pm 0.0016$ is still 3 standard deviations away from its SM value. The issue has been addressed in particular in the framework of the MSSM [2, 3, 4, 5, 6, 7, 8, 9]. It is well known already for some time that in the MSSM there are new contributions to the $Z^0\bar{b}b$ vertex which can significantly enhance the value of R_b (but not R_c) if some superpartners are sufficiently light [12, 2, 4, 5, 6, 8, 9]. More specifically, for low (large) $\tan\beta$ the dominant contributions are chargino–stop (CP –odd Higgs boson and chargino–stop) loops.

Any improvement in R_b must not destroy the perfect agreement of the SM with the other precision LEP measurements and must be consistent with several other experimental constraints (which will be listed later on). It is, therefore, important to discuss the changes in R_b in the context of global fits to the electroweak data (and with all additional constraints included). Such fits in the effective low energy MSSM (unconstrained by any GUT assumptions about the pattern of soft supersymmetry breaking scalar masses) have shown that it is realistic to obtain the values of R_b up to $R_b = 0.2180(0.2190)$ for small (large) $\tan\beta$ values [5]. Although still away by 1.5σ (1.0σ) even from the central experimental value obtained with R_c fixed to its SM value, those results provide an interesting improvement over the SM prediction $R_b = 0.2158$ (0.2160) for $m_t = 180$ (170) GeV. At the same time the overall best χ^2 is smaller than in the SM fits by $\Delta\chi^2 \approx 4$ (5 for the fit with R_c fixed to the SM value) (for $m_t = 170$ GeV). Also, the fitted value of $\alpha_s(M_Z)$ is modified by $\Delta\alpha_s(M_Z) \approx -4\delta R_b$, i.e. lower than in the SM fits which give $\alpha_s(M_Z) = 0.123 \pm 0.005$ [13, 3, 14, 10]. This may look desirable [7] in view of the apparent hint for some discrepancy between the value of $\alpha_s(M_Z)$ obtained from the SM fits to the precision electroweak data and the values $\alpha_s(M_Z) = 0.112 \pm 0.005$ and $\alpha_s(M_Z) = 0.112 \pm 0.007$ obtained from the deep inelastic scattering [15] and lattice calculations [16], respectively ¹. Furthermore, increase of R_b in the MSSM implies some light

¹The overall average gives $\alpha_s(M_Z) = 0.117 \pm 0.005$ and includes also the results

superpartners, with masses of the order or even below the electroweak scale M_Z [4, 5, 6, 18] ! (It is may be worth noting small differences between various viewpoints: One is to explain the measured value of R_b . The other is to take it as a statistical hint for values of R_b somewhat higher then predicted by the SM. It is reasonable to take the latter and to consider an increase in R_b in the range 0.2170–0.2180(90) as interesting.)

In this paper, encouraged by the importance of the R_b anomaly for experimental search for supersymmetry, we take up this issue once again. We clarify certain points of the earlier analysis and provide further insight into properties of light superpartners predicted by such global fits. Furthermore, we clarify the rôle of various experimental constraints, including the recent new limits on the chargino mass from LEP1.5. Our main new result is that for low $\tan\beta$ the χ^2 of the global fit and the value of R_b depend very weakly on the chargino mass (for fixed stop mass) in the range 50–100 GeV. The R_b remains at the level of 0.2178 for m_{C_1} up to 90 GeV in the region where $M_2 \sim |\mu|$ and $\mu < 0$. We also discuss large $\tan\beta$ case.

2. LOW $\tan\beta$ REGION.

Our discussion will be divided into small and large $\tan\beta$ cases. To start with, let us, however, recall the basic facts from the global fits in the MSSM. In order to maintain good agreement of the SM with the bulk of the precision data, such as $\Delta\rho$, M_W , $\sin^2\theta_{lept}^{eff}$, ... we must avoid new sources of the custodial $SU_V(2)$ symmetry breaking in the left currents. In the MSSM, this is assured when the left squarks of the third generation (and all left sleptons) are sufficiently heavy [19, 5], say, $> \mathcal{O}(500 \text{ GeV})$ ². At the same time, an increase in R_b requires a light right stop. So, one needs a hierarchy³:

$$M_{\tilde{t}_L} \gg M_{\tilde{t}_R} \quad \text{or} \quad M_{\tilde{t}_1} \gg M_{\tilde{t}_2} \quad (1)$$

(in our notation \tilde{t}_2 denotes the lighter stop) with small left-right mixing.

The second important fact to recall is the pattern of the chargino sector (masses and mixings). The chargino mass matrix

$$\mathcal{L}_{mass} = -\frac{1}{2}(\chi^+, \chi^-) \begin{pmatrix} 0 & X^T \\ X & 0 \end{pmatrix} \begin{pmatrix} \chi^+ \\ \chi^- \end{pmatrix} + h.c. \quad (2)$$

with

$$X = \begin{pmatrix} M_2 & \sqrt{2}M_W \sin\beta \\ \sqrt{2}M_W \cos\beta & \mu \end{pmatrix} \quad (3)$$

obtained from τ decay and jet physics [17]

²The actual lower limits on left squarks and sleptons depend on $\tan\beta$ value [19, 5].

³Such a hierarchy is very natural in models where soft scalar mass terms have their origin at the GUT scale. Even with universal initial squark mass values m_0^2 , the renormalization group evolution with large top quark Yukawa coupling gives the hierarchy (1) provided $m_0^2 \gg M_2^2$

is diagonalized by two unitary matrices Z_+ and Z_- : $Z_-^T X Z_+ = \text{diag}(m_{C_1}, m_{C_2})$ with $0 < m_{C_1} < m_{C_2}$ (we follow the convention and notation of ref. [20]) which determine the projection of the physical two-component states λ_i^\pm ($i = 1, 2$) on the gaugino and higgsino two-component weak eigenstates $(-i\psi^+, h_2^+, -i\psi^-, h_1^-) \equiv (\chi^+, \chi^-)$

$$h_2^+ = Z_+^{2i} \lambda_i^+, \quad h_1^- = Z_-^{2i} \lambda_i^- \quad (4)$$

$$\psi^\pm = i Z_\pm^{1i} \lambda_i^\pm \quad (5)$$

with the Dirac charginos defined as

$$C_i^- = \begin{pmatrix} \lambda_i^- \\ \lambda_i^+ \end{pmatrix} \quad (6)$$

It is important to notice that a physical state C_i^- may contain different admixtures of the "up" and "down" higgsinos (h_2 and h_1 respectively). For instance, it may be almost pure up-higgsino (in which case $|Z_+^{2i}| \gg |Z_+^{1i}|$) in its lower two-component spinor λ_i^+ and almost pure gaugino ($|Z_-^{2i}| \ll |Z_-^{1i}|$) in its upper two-component spinor λ_i^- . For small values of $\tan \beta$ the pattern of the gaugino-higgsino mixing in the physical states is not just determined by the ratio $r \equiv M_2/|\mu|$ but also crucially depends on the sign of μ . In addition, for fixed M_2 and μ also the pattern of the physical masses depends on the sign of μ in a crucial way as shown in Fig.1. For better qualitative understanding of those points it is instructive to consider the chargino masses and mixing for $r = 1$. For both signs of the μ parameter and any value of $\tan \beta$ the chargino mass matrix (3) can be easily transformed into symmetric form which is diagonalized by an unitary (orthogonal in our case of real μ and M_2) matrix i.e. $Z'_+ = Z'_-$. With both eigenvalues positive and ordered, $m_{C_1} < m_{C_2}$, (we use the fact that $\tan \beta > 1$), the complete diagonalizing matrices read:

for $\mu > 0$

$$Z_- = \begin{pmatrix} -c_\theta & s_\theta \\ s_\theta & c_\theta \end{pmatrix} \quad Z_+ = \begin{pmatrix} -s_\theta & c_\theta \\ c_\theta & s_\theta \end{pmatrix} \quad (7)$$

for $\mu < 0$

$$Z_- = \begin{pmatrix} s_\theta & -c_\theta \\ c_\theta & s_\theta \end{pmatrix} \quad Z_+ = \begin{pmatrix} c_\theta & -s_\theta \\ -s_\theta & -c_\theta \end{pmatrix} \quad (8)$$

where $s_\theta \equiv \sin \theta$, $c_\theta \equiv \cos \theta$. For the angle θ we get for $\mu > 0$

$$\tan 2\theta = -\frac{2\mu}{\sqrt{2}M_W(\sin \beta - \cos \beta)} < 0 \quad (9)$$

for $\mu < 0$

$$\tan 2\theta = -\frac{2\mu}{\sqrt{2}M_W(\sin\beta + \cos\beta)} > 0 \quad (10)$$

We see that for low values of $\tan\beta$ the two cases are very different. For $\mu > 0$ we get $\theta \sim \pi/4$ and $c_\theta \sim s_\theta \sim 1/\sqrt{2}$. Thus all two-component states are mixed. Moreover, the mass eigenstates are

$$m_{C_{1,2}} = \mu \mp \frac{1}{\sqrt{2}}M_W(\sin\beta + \cos\beta) + \frac{1}{4}(1 - \sin 2\beta)\frac{M_W^2}{\mu} + \dots \quad (11)$$

for $\mu > M_W$ (smaller μ values are excluded by experimental constraints) and charginos are split in mass by $\Delta m_C \sim 2M_W$. Pure up-higgsino can only be obtained for $r \gg 1$. One can then check that the lighter chargino is higgsino-like in both two-component spinors i.e. $|Z_\pm^{21}\rangle \gg |Z_\pm^{11}\rangle$ and the second chargino is heavy.

For $\mu < 0$ and $|\mu| \ll M_W$ we get $\theta \sim 0$ and $c_\theta \sim 1$. The mass eigenvalues for low $\tan\beta$ are

$$\begin{aligned} m_{C_1} &= \sqrt{2}\cos\beta M_W \left(1 + \frac{1}{2\cos\beta(\sin\beta + \cos\beta)}\frac{\mu^2}{M_W} + \dots \right) \\ m_{C_2} &= \sqrt{2}\sin\beta M_W \left(1 + \frac{1}{2\sin\beta(\sin\beta + \cos\beta)}\frac{\mu^2}{M_W} + \dots \right) \end{aligned} \quad (12)$$

First of all, low values of μ are indeed allowed for $m_{C_1} > 65$ GeV and the heavier chargino is still very light. Moreover, the heavier chargino is pure up-higgsino (gaugino) in its lower (upper) two-component spinor. For large values of r and/or large values of $\tan\beta$ the difference between $\mu > 0$ and $\mu < 0$ disappears.

We can study now the supersymmetric contributions to the $Z^0\bar{b}b$ vertex. In the low $\tan\beta$ region there are two types of relevant diagrams: with stop coupled to Z^0 and with charginos coupled to Z^0 . Their (renormalized) contributions to the vector and axial-vector formfactors of the $Z^0\bar{b}b$ vertex F_V and F_A ($\mathcal{L}_{Z^0\bar{b}b}^{eff} = \bar{\psi}_b\gamma^\mu(F_V - \gamma^5 F_A)\psi_b Z_\mu^0$) are (in the limit $m_b = 0$) given by (the sum is over the two stop and two chargino mass eigenstates):

$$\begin{aligned} \delta F_V^{(\hat{t})} &= \frac{e}{4s_W c_W} \sum_{n,m,l} V_{Z\hat{t}\hat{t}}^{l,n} \left(L_{\hat{b}\hat{t}C}^{l,m*} L_{\hat{b}\hat{t}C}^{n,m} + R_{\hat{b}\hat{t}C}^{l,m*} R_{\hat{b}\hat{t}C}^{n,m} \right) \\ &\quad \times f_{ssf}(M_Z^2; M_{\hat{t}_n}, m_{C_m}, M_{\hat{t}_l}) \end{aligned} \quad (13)$$

$$\begin{aligned} \delta F_A^{(\hat{t})} &= \frac{e}{4s_W c_W} \sum_{n,m,l} V_{Z\hat{t}\hat{t}}^{l,n} \left(L_{\hat{b}\hat{t}C}^{l,m*} L_{\hat{b}\hat{t}C}^{n,m} - R_{\hat{b}\hat{t}C}^{l,m*} R_{\hat{b}\hat{t}C}^{n,m} \right) \\ &\quad \times f_{ssf}(M_Z^2; M_{\hat{t}_n}, m_{C_m}, M_{\hat{t}_l}) \end{aligned} \quad (14)$$

$$\begin{aligned}
\delta F_V^{(C)} &= \frac{e}{4s_W c_W} \sum_{n,m,l} \left(R_{ZCC}^{m,l} L_{b\tilde{t}C}^{n,l*} L_{b\tilde{t}C}^{n,m} + L_{ZCC}^{m,l} R_{b\tilde{t}C}^{n,l*} R_{b\tilde{t}C}^{n,m} \right) \\
&\quad \times m_{C_m} m_{C_l} c_0(m_{C_m}, M_{\tilde{t}_n}, m_{C_l}) \\
&- \frac{e}{4s_W c_W} \sum_{n,m,l} \left(L_{ZCC}^{m,l} L_{b\tilde{t}C}^{n,l*} L_{b\tilde{t}C}^{n,m} + R_{ZCC}^{m,l} R_{b\tilde{t}C}^{n,l*} R_{b\tilde{t}C}^{n,m} \right) \\
&\quad \times f_{ffs}(M_Z^2, m_{C_m}, M_{\tilde{t}_n}, m_{C_l})
\end{aligned} \tag{15}$$

$$\begin{aligned}
\delta F_A^{(C)} &= \frac{e}{4s_W c_W} \sum_{n,m,l} \left(R_{ZCC}^{m,l} L_{b\tilde{t}C}^{n,l*} L_{b\tilde{t}C}^{n,m} - L_{ZCC}^{m,l} R_{b\tilde{t}C}^{n,l*} R_{b\tilde{t}C}^{n,m} \right) \\
&\quad \times m_{C_m} m_{C_l} c_0(m_{C_m}, M_{\tilde{t}_n}, m_{C_l}) \\
&- \frac{e}{4s_W c_W} \sum_{n,m,l} \left(L_{ZCC}^{m,l} L_{b\tilde{t}C}^{n,l*} L_{b\tilde{t}C}^{n,m} - R_{ZCC}^{m,l} R_{b\tilde{t}C}^{n,l*} R_{b\tilde{t}C}^{n,m} \right) \\
&\quad \times f_{ffs}(M_Z^2, m_{C_m}, M_{\tilde{t}_n}, m_{C_l})
\end{aligned} \tag{16}$$

where s_W , c_W stand for $\sin \theta_W$, $\cos \theta_W$ and the finite functions f_{ssf} , f_{ffs} and c_0 are defined in the Appendix B. The couplings read [20]:

$$V_{Z\tilde{t}\tilde{t}}^{l,n} = T^{1l} T^{1n} - \frac{4}{3} \sin^2 \theta_W \delta^{ln} \tag{17}$$

$$\begin{aligned}
L_{ZCC}^{m,l} &= Z_+^{1m*} Z_+^{1l} + \delta^{ml} \cos 2\theta_W, \\
R_{ZCC}^{m,l} &= Z_-^{1m} Z_-^{1l*} + \delta^{ml} \cos 2\theta_W
\end{aligned} \tag{18}$$

$$\begin{aligned}
L_{b\tilde{t}C}^{n,l} &= \frac{e}{s_W} T^{1n} Z_+^{1l} - \frac{e}{\sqrt{2}s_W c_W} \frac{m_t}{M_Z \sin \beta} T^{2n} Z_+^{2l}, \\
R_{b\tilde{t}C}^{n,l} &= -\frac{e}{\sqrt{2}s_W c_W} \frac{m_b}{M_Z \cos \beta} T^{1n} Z_-^{2l*}
\end{aligned} \tag{19}$$

The top squark mixing matrix T^{ij} is defined by:

$$\begin{pmatrix} \tilde{t}_L \\ \tilde{t}_R \end{pmatrix} = \begin{pmatrix} T^{11} & T^{12} \\ T^{21} & T^{22} \end{pmatrix} \begin{pmatrix} \tilde{t}_1 \\ \tilde{t}_2 \end{pmatrix} = \begin{pmatrix} c_t & -s_t \\ s_t & c_t \end{pmatrix} \begin{pmatrix} \tilde{t}_1 \\ \tilde{t}_2 \end{pmatrix} \tag{20}$$

where $s_t \equiv \sin \theta_t$, $c_t \equiv \cos \theta_t$. In the case of small $\tan \beta$ the couplings $R_{b\tilde{t}C}^{n,l}$ are negligible and we have $\delta F_V = \delta F_A$. When the lighter stop, \tilde{t}_2 , is dominantly right-handed, as required for a large $b\tilde{t}_2 C$ coupling, its coupling to Z^0 is suppressed (it is proportional to $g \sin^2 \theta_W$). Therefore, diagrams with stops coupled directly to Z^0 cannot give any significant enhancement of R_b . Significant contribution can only come from diagrams in which charginos are coupled to Z^0 . Their actual magnitude depend on

the interplay of the couplings in the $C_i^- \tilde{t}_2 b$ vertex and the $Z^0 C_i^- C_j^-$ vertex. The first one is large only for charginos with large up-higgsino component, the second - for charginos with large gaugino component in at least one of its two-component spinors. As we have seen, this combination never happens for $\mu > 0$. Large R_b can then only be achieved at the expense of extremely light C_j^- and \tilde{t}_2 , either already ruled out by the existing mass limits or in conflict with global χ^2 and/or other constraints such as $BR(b \rightarrow s\gamma)$, $BR(t \rightarrow new)$. In addition, for fixed m_{C_1} and $M_{\tilde{t}_2}$, R_b is larger for $r > 1$ i.e. for higgsino-like chargino as the enhancement of the $C_1^- \tilde{t}_2 b$ coupling is more important than of the $Z^0 C_1^- C_1^-$ coupling.

For $\mu < 0$ the situation is much more favourable. In the range $r \approx 1 \pm 0.5$ the second chargino which for low $\tan\beta$, is very close in mass to the lighter one (Fig.1), has large up-higgsino component and gaugino component. Large couplings in both types of vertices of the diagram with charginos coupled to Z^0 give significant increase in R_b even for the lighter chargino as heavy as 80 – 90 GeV (similar increase in R_b for $\mu > 0$ requires $m_{C_1} \approx 50$ GeV and $M_{\tilde{t}_2} \approx 50$ GeV).

We now turn our attention to a global fit to the precision data and to the rôle of the following constraints: 1) $\Gamma(Z^0 \rightarrow \chi_1^0 \chi_1^0) < 4$ MeV (in addition to the inclusion of the decay mode $Z^0 \rightarrow \chi_i^0 \chi_j^0$ into the total Z^0 width in the χ^2 fit), 2) $BR(Z^0 \rightarrow \chi_1^0 \chi_2^0) < 10^{-4}$, 3) $M_h > 60$ (50) GeV for small (large) $\tan\beta$, 4) $BR(b \rightarrow s\gamma)$ in the range $(1.2 - 3.4) \times 10^{-4}$ 5) $BR(t \rightarrow new) < 45\%$ (following ref. [21])⁴. 6) Recent exclusion curves in the $(m_{N_1}, M_{\tilde{t}_2})$ plane from $D0$ obtained under the assumption $m_{C_1} > M_{\tilde{t}_2}$ [23]. Since the uncertainty in most of these constraints is much larger than in the precision data, we perform the χ^2 fit to the latter and impose the former as rigid constraints. Importance of the constraints is illustrated in Figs. 2 and 3 and should be discussed in more detail.

The limits $\Gamma(Z^0 \rightarrow \chi_1^0 \chi_1^0) < 4$ MeV and $BR(Z^0 \rightarrow \chi_1^0 \chi_2^0) < 10^{-4}$ put a constraint on the (M_2, μ) parameter space provided we make an additional assumption about the values of M_1 (bino mass). In this paper, for a sake of definiteness, we adopt the GUT relation $M_1 = (5/3) \tan^2 \theta_W M_2$. Then for low $\tan\beta$ the two constraints eliminate (approximately) a band in the M_2, μ plane bounded by $-50 < \mu < 100$ GeV. This is basically due to the fact that for M_2 and μ in this region neutralinos are too light and/or have too strong coupling to Z^0 . The values of M_2 and μ chosen for Figs. 2,3 (and 7) are outside the forbidden region. One should remember, however, that the limits on $Z^0 \rightarrow N_1^0 N_1^0$ and $Z^0 \rightarrow N_1^0 N_2^0$ are less constraining for larger values of M_1 , $M_1 > 0.5M_2$ (i.e. heavier LSP). Similarly, the

⁴This is a constraint mainly on the decay $t \rightarrow \tilde{t}_2 N_i^0$. In the large $\tan\beta$ case, an important decay can also be $t \rightarrow bH^+$, with M_{H^\pm} close to M_W . It is difficult to distinguish this decay mode from the standard one, $t \rightarrow bW^+$ [22] and to put an experimental upper bound on this branching ratio.

bounds on $M_{\tilde{t}_2}$ from the $D0$ exclusion curves gradually disappear for $M_1 > 0.5M_2$. Finally, the larger the M_1 the better the degeneracy between the lighter chargino and the lightest neutralino masses. This is important since the new LEP1.5 limit $m_{C_1} > 65$ GeV has been obtained under the assumption $m_{C_1} - m_{N_1^0} > 10$ GeV [24]. We see that the significance of various constraints crucially depends on the ratio M_1/M_2 . With the GUT assumption, our results remain on the conservative side.

The rôle of the lower limit on the Higgs boson mass (for a compact formula for radiatively corrected lighter Higgs boson mass in the limit $M_A \gg M_Z$ see [25]) depends on the mass of the heavier stop and the left-right mixing angle. For $M_{\tilde{t}_1} > 500$ GeV (as required for good quality of the global fit) and small mixing angles (necessary for large R_b) M_h is above the experimental limit ⁵ in a large range of the parameter space. Very small and large left-right mixing angles are, however, ruled out by this constraint. This is clearly seen in Figs. 2 and 3 where we show the allowed region in the $(M_{\tilde{t}_2}, \theta_t)$ plane for fixed M_2, μ and $\tan\beta$.

The $b \rightarrow s\gamma$ decay is a very important constraint on the parameters space. In addition to the experimental error in the $BR(b \rightarrow s\gamma)$ (which we take at the 2σ level) there is large uncertainty in the theoretical prediction mainly due to its renormalization scale dependence [26]. In Figs. 2 and 3 we show the significance of the $b \rightarrow s\gamma$ constraint in two cases: when the renormalization scale Q is fixed, $Q = m_b = 4.7$ GeV and with the theoretical uncertainty included. In the latter case we consider the result for the $BR(b \rightarrow s\gamma)$ as acceptable if any of the theoretical values obtained with Q varying from $m_b/2$ to $2m_b$ falls into the 2σ experimental range. Moreover, the results for $BR(b \rightarrow s\gamma)$ show weak but nonnegligible dependence on the value of $\alpha_s(M_Z)$. Since the fitted value $\alpha_s(M_Z)$ depends on the change in R_b , in Figs. 2 and 3 for self-consistency we use the value $\alpha_s(M_Z) = 0.123 + \delta\alpha_s$ where $\delta\alpha_s = -4\delta R_b$ and the value 0.123 is obtained from the SM fit [13, 3, 14, 10]. For comparison, in Fig. 2, we also show the regions excluded by this constraint with $\alpha_s(M_Z)$ fixed to two different values 0.114 and 0.135. An important message from Figs. 2 and 3 is the dependence of the $b \rightarrow s\gamma$ constraint on the left-right mixing in the stop sector. One should stress that we keep the mass of the CP -odd Higgs boson large, $M_A = 1$ TeV (as needed for large R_b) and in consequence the charged Higgs boson is also heavy and its exchange gives negligible contribution to the $BR(b \rightarrow s\gamma)$. The acceptable values of this branching ratio are obtained from the sum $|\mathcal{A}_W^{b \rightarrow s\gamma} + \mathcal{A}_{SU,SY}^{b \rightarrow s\gamma}|$ of the SM W^\pm exchange and the supersymmetric contribution of the $\tilde{t} - C^-$ loops which has to be of the opposite sign. There are two possible solutions: either

⁵Important rôle of the experimental lower bound on M_h in ref. [9] in constraining the potential increase of R_b is due to the chosen upper bound $M_{\tilde{t}_1} < 250$ GeV which, anyway, looks too low from the point of view of global fit.

$|\mathcal{A}_{SUSY}^{b \rightarrow s\gamma}| \ll |\mathcal{A}_W^{b \rightarrow s\gamma}|$ or $|\mathcal{A}_{SUSY}^{b \rightarrow s\gamma}| \gg |\mathcal{A}_W^{b \rightarrow s\gamma}|$. The strong dependence of the supersymmetric contribution to the $b \rightarrow s\gamma$ rate on the mixing angle θ_t observed in Fig. 2 and 3 can be understood from the general formulae given in [27]. For $r = 1$ and small angles θ_t (interesting values of ΔR_b are obtained only for small mixing angles θ_t ; large angles are anyway eliminated by the constraint from the lighter Higgs boson mass), setting $\sin^2 \theta_t \approx 0$, neglecting the contribution of the heavier stop \tilde{t}_1 and using the explicit form of the matrices Z_+ and Z_- , eqs. (7,8), we get the expression:

$$\begin{aligned} \mathcal{A}_{\gamma/gl, SUSY}^{b \rightarrow s\gamma} &= -g_t^2 c_\theta^2 \frac{M_W^2}{m_{C_1}^2} f_{\gamma/gl}^{(1)} \left(\frac{M_{\tilde{t}_2}^2}{m_{C_1}^2} \right) - g_t^2 s_\theta^2 \frac{M_W^2}{m_{C_2}^2} f_{\gamma/gl}^{(1)} \left(\frac{M_{\tilde{t}_2}^2}{m_{C_2}^2} \right) \\ &+ \sin 2\theta_t s_\theta c_\theta g_t \left[\frac{M_W^2}{m_{C_1}^2} f_{\gamma/gl}^{(1)} \left(\frac{M_{\tilde{t}_2}^2}{m_{C_1}^2} \right) + \sigma \frac{M_W^2}{m_{C_2}^2} f_{\gamma/gl}^{(1)} \left(\frac{M_{\tilde{t}_2}^2}{m_{C_2}^2} \right) \right. \\ &\left. + \sigma \frac{M_W}{2m_{C_1}} f_{\gamma/gl}^{(3)} \left(\frac{M_{\tilde{t}_2}^2}{m_{C_1}^2} \right) + \sigma \frac{M_W}{2m_{C_2}} f_{\gamma/gl}^{(3)} \left(\frac{M_{\tilde{t}_2}^2}{m_{C_2}^2} \right) \right] \end{aligned} \quad (21)$$

where $\sigma \equiv \text{sign}(\mu)$, $g_t \equiv m_t/\sqrt{2}M_W \sin \beta$ and the expressions for the functions $f_{\gamma/gl}^{(i)}(x)$ can be found in [27]. Recalling that, for the same values of the arguments, functions $f_{\gamma/gl}^{(3)}(x)$ are roughly 5 times larger in absolute values than the $f_{\gamma/gl}^{(1)}(x)$'s (and both are negative) it is easy to see that for $\mu > 0$ $\mathcal{A}_{SUSY}^{b \rightarrow s\gamma}$ is small for $\theta_t > 0$ due to the cancellation of terms of order g_t^2 with those of order g_t . For small negative θ_t both types of terms add up and cancel with the standard W^\pm contribution making the total amplitude unacceptably small. Eventually, for large negative angles, the supersymmetric contribution overcomes the standard one making again the total amplitude of right magnitude. However this region is excluded by the experimental limits on the Higgs boson mass. For negative μ the cancelation between terms of order g_t^2 and those of order g_t , which makes $\mathcal{A}_{SUSY}^{b \rightarrow s\gamma}$ small enough, occurs for negative angles θ_t . For positive angles the supersymmetric contribution is large and cancels the standard one making the total amplitude too small.

Thus, there are two mechanisms for obtaining an acceptable value for $BR(b \rightarrow s\gamma)$ in the MSSM. One is a cancellation between the H^\pm and supersymmetric contributions [29]. This mechanism is, however, essentially in conflict with the simultaneous increase of R_b due to large negative contribution of the H^\pm exchange to R_b . The other mechanism is based on the choice of the proper range of the left-right mixing angles. It is certainly interesting to notice that for small $\tan \beta$ the region of acceptable $BR(b \rightarrow s\gamma)$ partly overlaps with the region of large R_b . Small asymmetry (with respect to $\theta_t = 0$ of the constant ΔR_b^{SUSY} contours seen in Figs. 2 and 3 can also be traced back to the θ_t dependence of the couplings $L_{b\tilde{t}C}^{n,l}$ eqn. (19).

The exclusion curve from the condition $BR(t \rightarrow \tilde{t}_2 N_i^0) < 45\%$ is also

shown in Fig. 2. The dependence of $BR(t \rightarrow \tilde{t}_2 N_i^0)$ on the left - right mixing in the stop sector, i.e. on the angle θ_t , can be understood from the formula for the decay width $\Gamma(t \rightarrow \tilde{t}_2 N_i^0)$:

$$\begin{aligned} \Gamma(t \rightarrow \tilde{t}_k N_i^0) &= \frac{e^2}{s_W^2 c_W^2} \frac{m_t}{64\pi} \sqrt{1 - 2(x_k + y_i) + (x_k - y_i)^2} \\ &\times \left[(|c_L^{ki}|^2 + |c_R^{ki}|^2)(1 + y_i - x_k) + 4\mathcal{R}e(c_L^{ki*} c_R^{ki}) \sqrt{y_i} \right] \end{aligned} \quad (22)$$

where $x_k \equiv M_{\tilde{t}_k}^2/m_t^2$, $y_i \equiv m_{N_i}^2/m_t^2$ and the couplings read [20]:

$$\begin{aligned} c_L^{ki} &= \left(\frac{1}{3} s_W Z_N^{1i} + c_W Z_N^{2i} \right) T^{1k} + \frac{m_t}{\sin \beta M_Z} Z_N^{4i} T^{2k} \\ c_R^{ki} &= -\frac{4}{3} s_W Z_N^{1i} T^{2k} + \frac{m_t}{\sin \beta M_Z} Z_N^{4i} T^{1k} \end{aligned} \quad (23)$$

and Z_N^{ji} diagonalizes the neutralino mass matrix [20]. For example, for $\mu < 0$ and $r = 1$, $\Gamma(t \rightarrow new)$ is dominated by $\Gamma(t \rightarrow \tilde{t}_2 N_2^0)$ because the second neutralino has larger up-higgsino component. In that case

$$\begin{aligned} c_L^{22} &\approx \frac{m_t}{\sin \beta M_Z} Z_N^{42} \cos \theta_t \\ c_R^{22} &\approx -\frac{m_t}{\sin \beta M_Z} Z_N^{42} \sin \theta_t \end{aligned} \quad (24)$$

and

$$\begin{aligned} \Gamma(t \rightarrow \tilde{t}_2 N_2^0) &= \frac{e^2}{64\pi s_W^2 c_W^2} \frac{m_t^3}{M_Z^2 \sin^2 \beta} |Z_N^{42}|^2 \sqrt{1 - 2(x_2 + y_2) + (x_2 - y_2)^2} \\ &\times [(1 + y_2 - x_2) - 2 \sin 2\theta_t \sqrt{y_2}] \end{aligned} \quad (25)$$

explaining larger $BR(t \rightarrow new)$ for negative θ_t seen in Fig. 2.

The $D0$ exclusion contours [23] in the $(M_{\tilde{t}_2}, m_{N_1^0})$ plane eliminate in Fig. 2 a band $70 \text{ GeV} < M_{\tilde{t}_2} < m_{C_1}$ (not shown) and a similar band in Fig. 3. This follows from Fig. 10 in ref. [23] (in Fig. 2 $M_2 = -\mu = 58 \text{ GeV}$, $m_{C_1} = 85 \text{ GeV}$ and $m_{N_1} \approx 30 \text{ GeV}$ (with the GUT assumption)). Finally, it is worth recalling that

$$M_{\tilde{t}_2}^2 = M_{\tilde{t}_R}^2 - \theta_t^2 M_{\tilde{t}_L}^2, \quad |\theta_t| = \left| \frac{m_t A_t}{M_{\tilde{t}_L}^2} \right| \ll 1 \quad (26)$$

where

$$M_{\tilde{t}_R}^2 = m_T^2 + m_t^2 + \frac{2}{3} \cos 2\beta (M_Z^2 - M_W^2) \quad (27)$$

(m_T^2 is the soft supersymmetry breaking mass term). If we required $m_T^2 > 0$ then with $M_{\tilde{t}_L} \approx 1 \text{ TeV}$ we get $|\theta_t| > 9^\circ$ for $M_{\tilde{t}_2} \sim \mathcal{O}(100 \text{ GeV})$ and with

$M_{\tilde{t}_L} \approx 1.5$ TeV – $|\theta_t| > 6^\circ$. The corresponding values of A_t are ~ 1 TeV and ~ 600 GeV respectively. The theoretical status of the condition $m_T^2 > 0$ remains, however, unclear and we do not impose it on our global fit (with this condition imposed the fit would not have changed too significantly in particular given the freedom in the choice of $M_{\tilde{t}_L}$).

The results of a global fit are presented in Figs. 4-6 as projections of χ^2 as a function of m_{C_1} for several values of r and two different lower bounds for the scan in $M_{\tilde{t}_2}$. We also show the best values of R_b obtained with the restriction $\chi^2 < \chi_{min}^2 + 1$ where χ_{min}^2 is the minimum of the χ^2 for fixed m_{C_1} . The fitting procedure is the same as in ref. [5]. In particular the fitted parameters include m_t , $\tan\beta$, M_2 , μ , $\alpha_s(M_Z)$, $M_{\tilde{t}_2}$ and A_t . The values of the parameters $M_{\tilde{t}_L}$, M_{A^0} , $M_{\tilde{t}_L}$ provided large enough, are not relevant for the quality of the fit and we have fixed them at 1 TeV. Similarly, the parameters like $M_{\tilde{t}_R}$, $M_{\tilde{b}_R}$, masses and mixings of the two first generations of squarks to which the fit is not sensitive have been fixed at 1 TeV (in the large $\tan\beta$ case the best fit is obtained for $M_{\tilde{b}_R} = 130$ GeV due to additional contribution of $N_i^0 - \tilde{b}_R$ loops to R_b).

The value of $m_t = 170$ GeV chosen for the plots is close to the best value obtained from the fit. Larger values of m_t give worse χ^2 and this is a reflection of the well known from the SM fits correlation between the Higgs boson and the top quark masses [10, 14]. Here the M_h is constrained by supersymmetry and cannot follow the increase of m_t . In our fit $\tan\beta$ is bounded so that top quark Yukawa coupling remains perturbative up to the GUT scale (we take $\tan\beta \geq 1.4$ for $m_t = 170$ GeV and $\tan\beta \geq 1.6$ for $m_t = 180$ GeV). We impose this theoretical constraint to remain on the conservative side, as lower values of $\tan\beta$ (for the same m_t) give larger R_b . For a given m_t the best fit is obtained for the lowest value of $\tan\beta$ (for very large $\tan\beta$ see next section). One may also wish to impose the constraint $M_2 > 50$ GeV which follows from the lower experimental bound on the gluino mass $m_{\tilde{g}} > 150$ GeV and the assumed GUT relation for the gaugino masses. This constraint does not change the best values of R_b and χ^2 (but it eliminates e.g. large part of our curve with $r = 0.5$, $\mu < 0$).

All discussed earlier constraints are included in those results. The fit reveals several interesting facts. For both signs of μ , the value of χ^2 eventually increases towards low values of m_{C_1} . The reason for this behavior of χ^2 is the contribution of the neutralinos to Γ_Z which becomes too large and correspondingly σ_{hadr} - too small (at this point we should again remember about our assumption $M_1 = (5/3) \tan^2\theta_W M_2$). This effect is much stronger than the decrease of Γ_Z due to the chargino contribution to the Z^0 boson wave function renormalization [30]. So, the increase of R_b is bounded not only by the lower experimental limits on m_{C_1} , $M_{\tilde{t}_2}$ but also by the quality of the fit to the precision data. Still, for $\mu > 0$, the best fit is obtained for $m_{C_1} \sim 50$ GeV, well below the new experimental limit from

LEP1.5, $m_{C_1} > 65$ GeV [24]. This limit is valid for $m_{C_1} - m_{N_1} > 10$ GeV. In principle, the degeneracy of the chargino and neutralino masses can be better than 10 GeV. This occurs for $r > 10$ with $M_1 \approx 0.5M_2$ (note however, that supersymmetric contribution to R_b decreases for very large values of r) or for any value of r for sufficiently large M_1 . This is an obvious possibility which we do not discuss further. On the other hand, for $m_{C_1} = 65$ GeV the maximal reachable value of R_b is only $R_b = 0.2173$.

For $\mu < 0$ due to the mechanism explained earlier, $\chi^2(R_b)$ is small (large) for much larger values of m_{C_1} . In fact the new LEP1.5 limit is totally irrelevant in this case. A chargino with mass 70 – 90 GeV and with the composition described by $M_2 \approx |\mu|$ remains an interesting potential possibility. The dependence of R_b on the stop mass can be inferred from comparison of Fig. 4 and 5. We see that, even for $M_{\tilde{t}_2} = m_{C_1} = 90$ GeV, $R_b > 0.2175$. Moreover, a significant enhancement in R_b is consistent with both configurations: $M_{\tilde{t}_2} > m_{C_1}$ and $M_{\tilde{t}_2} < m_{C_1}$. In Fig. 1 we show the cross sections for chargino production as $\sqrt{s} = 190$ GeV. The corresponding cross sections for the production of the pair $N_1^0 N_2^0$ are also shown.

3. LARGE $\tan\beta$.

Significant enhancement of R_b is also possible for large $\tan\beta$ values, $\tan\beta \approx m_t/m_b$. In this case, in addition to the stop - chargino contribution there can be even larger positive contribution from the h^0 , H^0 and A^0 exchanges in the loops, provided those particles are sufficiently light (in this range of $\tan\beta$ $M_h \approx M_A$) and non-negligible sbottom-neutralino loop contributions. Recently it has been argued [8] that large $\tan\beta$ option of an enhancement in R_b is already ruled out by the constraints from $b \rightarrow c\tau\bar{\nu}_\tau$ and the absence of $4b$ events in the Z^0 decay which should have been present as a signature for the bremsstrahlung production of a light pseudoscalar Higgs boson A^0 at LEP1: $Z^0 \rightarrow \bar{b}bA^0 \rightarrow \bar{b}b\bar{b}b$. It has been claimed that the combination of the two constraints rules out the region in the $(M_A, \tan\beta)$ plane which can give substantial increase of R_b (see Fig. 2 in ref. [8]). It seems, however, that this conclusion cannot be maintained after proper account of experimental efficiencies in the search for the process $Z^0 \rightarrow \bar{b}b\bar{b}b$. The decay $b \rightarrow c\tau\bar{\nu}_\tau$ with $BR = 2.69 \pm 0.44$ % indeed puts an upper bound $\tan\beta < 0.52M_{H^\pm}/(1GeV)$ [32] which translates into a bound on M_A as a function of $\tan\beta$ which is given in ref. [8]. For instance, for $M_A = 55$ (65) GeV, allowed $\tan\beta < 63$ (68). However, with proper account of the experimental efficiency in search for $4b$ events and with 10^7 events from LEP1, one cannot expect to get for, say, $\tan\beta = 60$, a lower limit on M_A from this production mechanism better than about 40 GeV (since the four b tagging procedure is not 100% efficient, the

main source of the QCD background are $\bar{b}b g g$ and $\bar{b}b \bar{q} q$ final states)⁶. This is well below the reported limit of 55 GeV based on the analysis of the process $Z^0 \rightarrow A^0 h^0$ [33]. Thus, an enhancement of R_b in the large $\tan\beta$ region still remains an open possibility and we briefly summarize the relevant results.

The discussion of large $\tan\beta$ case is relatively simpler as most of the results is symmetric under the simultaneous change of sign of μ and θ_t . The contribution to the $Z^0 \bar{b}b$ vertex from chargino-stop loops to the vector and axial-vector formfactors are (in the limit $m_b = 0$) given by eqs. (13-17). Compact expressions for the remaining contributions are collected in Appendix A.

In the large $\tan\beta$ case, for both signs of μ the chargino composition is the same in the up and down Weyl spinors and is a monotonic function of the ratio r . For enhancement in R_b the $b\tilde{t}_2 C$ coupling is more important than the $Z^0 C C$ coupling, so higgsino-like chargino ($r \gg 1$) is more favourable. The chargino masses are then given by

$$\begin{aligned} m_{C_1} &\approx |\mu| \left(1 - \frac{M_W^2}{M_2^2} + \dots \right) \\ m_{C_2} &\approx M_2 \left(1 + \frac{M_W^2}{M_2^2} + \dots \right) \end{aligned} \quad (28)$$

The diagonalizing matrices have the form

$$Z_{\pm} = \begin{pmatrix} -\sin\theta_{\pm} & \cos\theta_{\pm} \\ \cos\theta_{\pm} & \sin\theta_{\pm} \end{pmatrix} \quad (29)$$

with

$$\tan 2\theta_- = \frac{2\sqrt{2}M_W\mu}{M_2^2 + 2M_W^2 - \mu^2}, \quad \tan 2\theta_+ = \frac{2\sqrt{2}M_W M_2}{M_2^2 - 2M_W^2 - \mu^2} \quad (30)$$

so that indeed for $M_2 \gg \mu, M_W$ both angles are close to zero. Notice however, that θ_+ (whose smallness is important for the coupling $b\tilde{t}_2 C$) approaches zero much slower than θ_- as r is increased. The rôle of the experimental constraints (listed in the previous section) on the parameter space is illustrated in Fig. 7. The regions ruled out by the $BR(b \rightarrow s\gamma)$ are easy to understand. Neglecting the contribution of the heavier chargino and stop and restricting to small angles θ_t in the general formula of [27] we get for the $b \rightarrow s\gamma$ amplitude the following expression

$$\mathcal{A}_{\gamma/gl, SUSY}^{b \rightarrow s\gamma} \approx -g_t^2 \cos^2\theta_+ \frac{M_W^2}{m_{C_1}^2} f_{\gamma/gl}^{(1)} \left(\frac{M_{\tilde{t}_2}^2}{m_{C_1}^2} \right)$$

⁶S. Simion and P. Janot, private communication. Such an experimental analysis has not yet been performed. We thank J. Kalinowski, M. Krawczyk, M. Carena and C. Wagner for several discussions of this point.

$$\begin{aligned}
& + \sin 2\theta_t \left(\frac{\tan \beta}{2\sqrt{2}} \right) g_t \cos \theta_+ \cos \theta_- \frac{M_W}{m_{C_1}} f_{\gamma/gl}^{(3)} \left(\frac{M_{\tilde{t}_2}^2}{m_{C_1}^2} \right) \\
& + \frac{1}{2} \frac{m_t^2}{M_{H^\pm}^2} f_{\gamma/gl}^{(2)} \left(\frac{m_t^2}{M_{H^\pm}^2} \right)
\end{aligned} \tag{31}$$

With very light A^0 , the charged Higgs boson contribution is large and adds up (with the same sign) to the standard W^\pm -top exchange amplitude. Thus we need a cancellation from the supersymmetric part of eq. (32). Due to the presence of large $\tan \beta$ factor, the second term is strongly dominant. Therefore, for $\theta_t \leq 0$ supersymmetric contribution to the $b \rightarrow s\gamma$ amplitude is of the opposite sign to the standard contribution. Moreover, for angles θ_t not very close to zero, the absolute value of the supersymmetric contribution exceeds the standard one. Thus, for a given chargino mass there are only two very narrow bands seen in Fig. 7 in the plane $(\theta_t, M_{\tilde{t}_2})$ where the total amplitude is acceptable: in the right one the total amplitude is of the same sign as the standard W^\pm -top and charged Higgs boson amplitudes and in the left band it is of the opposite sign. From the Figure 7 it is however clear that for large $\tan \beta$, the $b \rightarrow s\gamma$ rate does not constrain the value of R_b at all [5].

The lower experimental bound on the lightest Higgs boson mass in the large $\tan \beta$ scenario is ~ 40 GeV. Since in the MSSM $M_{A^0} \approx M_{h^0}$, our results are not constrained by this bound.

In the parameter space which gives enhancement in R_b , also the decays $t \rightarrow new$ are enhanced. In addition to $t \rightarrow \tilde{t}_2 N_i^0$, important is also the decay $t \rightarrow bH^+$. For instance, for $m_t = 170$ GeV, $\tan \beta = 50$, $m_{C_1} = 65$ GeV and $M_A = 55$ (65) GeV we get $BR(t \rightarrow bH^+)$ ranging from 37(34)% up to 49(46)% depending on the stop sector parameters. One should remember, however, that the decay $t \rightarrow bH^+$ is not easily distinguishable from the standard one, $t \rightarrow bW^+$, for M_{H^+} close to M_W [22] and we do not impose this constraint in the global fit.

In Figs. 8 and 9 we present the results of a global fit in the large $\tan \beta$ case, together with the corresponding values of R_b . Two important features of the global χ^2 is the strong decrease in the quality of the fit for $m_t = 180$ GeV (compared to the best fit for $m_t = 170$ GeV) and for light charginos (below 60 GeV). Those effects are stronger than similar effects for low $\tan \beta$.

The values of R_b are almost insensitive to the value of $M_{\tilde{t}_2}$ in the range 50–100 GeV and show the expected dependence on M_A and m_{C_1} with the maximal values for very light charginos. It is, therefore, worth recalling that the new limit $m_{C_1} > 65$ GeV is based on the assumption $m_{C_1} - m_{N_1} > 10$ GeV. As for low $\tan \beta$, better degeneracy of the two masses can be achieved for $r > 10$ and/or for $M_1 > 0.5M_2$. In this case also the quality of the fit with charginos below 65 GeV is improved as heavier neutralinos contribute less to Γ_Z . It is also remarkable, that due to the combined effect of neutral

Higgs exchange and the chargino-stop together with the neutralino - sbottom contributions, the R_b remains greater than 0.2175 for masses well above the present experimental limits. E.g., for $m_{C_1} \approx M_{\tilde{t}_2} \approx M_A \approx 70$ GeV, $R_b = 0.2178$.

4. CONCLUSIONS.

In this paper we re-examined the possible magnitude of the supersymmetric contributions to R_b , with imposed all available phenomenological constraints and demanding good quality of the global fit to the precision electroweak data. For low $\tan\beta$ we have found a new region of the parameter space, with $M_2 \approx |\mu|$ and $\mu < 0$ where R_b remains large, ~ 0.2180 , even for the lighter chargino as heavy as 90 GeV. It is an interesting mixture of the up-higgsino and gaugino. The rôle of various phenomenological constraints is discussed in detail in analitic form and importance of small but *non-negligible* left-right mixing in the stop sector is emphasized in this context.

The large $\tan\beta$ option for enhancement of R_b is also summarized, with similar conclusions to those presented in the earlier papers. The available data do not rule out the possibility of large R_b in the large $\tan\beta$ case.

We conclude that the new LEP1.5 limit, $m_{C_1} > 65$ GeV still leaves open the possibility of a supersymmetric explanation of R_b up to 0.2180. We also conclude that $R_b > 0.2175$ even for $m_{C_1} = M_{\tilde{t}_2} = 90$ GeV both in small $\tan\beta$ and large $\tan\beta$ cases. Thus LEP2 may not resolve this question.

Finally, we stress that a good quality of the global fit requires the hierarchy $M_{\tilde{t}_2} \ll M_{\tilde{t}_1}$ (i.e. $M_{\tilde{t}_R} \ll M_{\tilde{t}_L}$). This hierarchy is natural if the low energy values of the soft squark masses have their origin in the renormalization group evolution from the GUT scale with the initial condition $m_0^2 \gg M_2^2$.

Acknowledgments: We are grateful to M. Olechowski for an independent check of our numerical code for δR_b^{SU5Y} and to W. de Boer for communicating to us his unpublished results which agree with ours. We would also like to thank R. Hempfling for discussion. P.H. Ch. would like to thank Max-Planck-Institut für Physik for warm hospitality during his stay in Munich where part of this work was done.

APPENDIX A.

Here we collect formulae for the remaining contributions to the $Z^0\bar{b}b$ vertex.

The contribution from charged Higgs boson is given by:

$$\begin{aligned}\delta F_V^{(t)} &= \frac{e^3}{8s_W^3 c_W^3} \left[\left(1 - \frac{4}{3}s_W^2\right) X_b - \frac{4}{3}s_W^2 X_t \right] f_{ffs}(M_Z^2; m_t, M_{H^\pm}, m_t) \\ &\quad - \frac{e^3}{8s_W^3 c_W^3} \left[\left(1 - \frac{4}{3}s_W^2\right) X_t - \frac{4}{3}s_W^2 X_b \right] m_t^2 c_0(m_t, M_{H^\pm}, m_t)\end{aligned}\quad (32)$$

$$\begin{aligned}\delta F_A^{(t)} &= -\frac{e^3}{8s_W^3 c_W^3} \left[\left(1 - \frac{4}{3}s_W^2\right) X_b + \frac{4}{3}s_W^2 X_t \right] f_{ffs}(M_Z^2; m_t, M_{H^\pm}, m_t) \\ &\quad - \frac{e^3}{8s_W^3 c_W^3} \left[\left(1 - \frac{4}{3}s_W^2\right) X_t + \frac{4}{3}s_W^2 X_b \right] m_t^2 c_0(m_t, M_{H^\pm}, m_t)\end{aligned}\quad (33)$$

$$\delta F_V^{(H^\pm)} = -\frac{e^3}{8s_W^3 c_W^3} (1 - 2s_W^2) (X_b + X_t) f_{ssf}(M_Z^2; M_{H^\pm}, m_t, M_{H^\pm})\quad (34)$$

$$\delta F_A^{(H^\pm)} = \frac{e^3}{8s_W^3 c_W^3} (1 - 2s_W^2) (X_b - X_t) f_{ssf}(M_Z^2; M_{H^\pm}, m_t, M_{H^\pm})\quad (35)$$

where we used the abbreviations

$$X_b \equiv \left(\frac{m_b}{M_Z} \tan \beta\right)^2, \quad X_t \equiv \left(\frac{m_t}{M_Z} \cot \beta\right)^2\quad (36)$$

As is well known, contribution of the charged Higgs boson to R_b is negative [12]. Positive contribution to R_b is provided by the neutral Higgs bosons.

$$\delta F_V^{(b, A^0)} = -\frac{e^3}{16s_W^3 c_W^3} \left(1 - \frac{4}{3}s_W^2\right) X_b f_{ffs}(M_Z^2; m_b, M_{A^0}, m_b)\quad (37)$$

$$\delta F_A^{(b, A^0)} = \frac{e^3}{16s_W^3 c_W^3} X_b f_{ffs}(M_Z^2; m_b, M_{A^0}, m_b)\quad (38)$$

$$\begin{aligned}\delta F_V^{(b, H^0, h^0)} &= -\frac{e^3}{16s_W^3 c_W^3} \left(1 - \frac{4}{3}s_W^2\right) X_b \left[\cos^2 \alpha f_{ffs}(M_Z^2; m_b, M_{H^0}, m_b) \right. \\ &\quad \left. + \sin^2 \alpha f_{ffs}(M_Z^2; m_b, M_{h^0}, m_b) \right]\end{aligned}\quad (39)$$

$$\delta F_A^{(b,H^0,h^0)} = \frac{e^3}{16s_W^3 c_W^3} X_b \left[\cos^2 \alpha f_{ffs}(M_Z^2; m_b, M_{H^0}, m_b) + \sin^2 \alpha f_{ffs}(M_Z^2; m_b, M_{h^0}, m_b) \right] \quad (40)$$

$$\delta F_V^{(b,A^0,H^0,h^0)} = 0 \quad (41)$$

$$\delta F_A^{(b,A^0,H^0,h^0)} = -\frac{e^3}{4s_W^3 c_W^3} X_b \left[\cos^2 \alpha f_{ssf}(M_Z^2; M_{A^0}, m_b, M_{H^0}) + \sin^2 \alpha f_{ssf}(M_Z^2; M_{A^0}, m_b, M_{h^0}) \right] \quad (42)$$

where α is the neutral CP -even Higgs bosons mixing angle [31].

For completeness we display also formulae for the neutralino - sbottom contribution.

$$\delta F_V^{(\tilde{b})} = -\frac{e}{4s_W c_W} \sum_{n,m,l} V_{Z\tilde{b}\tilde{b}}^{l,m} \left(L_{\tilde{b}\tilde{b}N}^{m,n*} L_{\tilde{b}\tilde{b}N}^{l,n} + R_{\tilde{b}\tilde{b}N}^{m,n*} R_{\tilde{b}\tilde{b}N}^{l,n} \right) \times f_{ssf}(M_Z^2; M_{\tilde{b}_m}, m_{N_n}, M_{\tilde{b}_l}) \quad (43)$$

$$\delta F_A^{(\tilde{b})} = -\frac{e}{4s_W c_W} \sum_{n,m,l} V_{Z\tilde{b}\tilde{b}}^{l,m} \left(L_{\tilde{b}\tilde{b}N}^{m,n*} L_{\tilde{b}\tilde{b}N}^{l,n} - R_{\tilde{b}\tilde{b}N}^{m,n*} R_{\tilde{b}\tilde{b}N}^{l,n} \right) \times f_{ssf}(M_Z^2; M_{\tilde{b}_m}, m_{N_n}, M_{\tilde{b}_l}) \quad (44)$$

$$\begin{aligned} \delta F_V^{(N)} &= -\frac{e}{2s_W c_W} \sum_{n,m,l} \left(R_{ZNN}^{l,m} L_{\tilde{b}\tilde{b}N}^{n,l*} L_{\tilde{b}\tilde{b}N}^{n,m} + L_{ZNN}^{l,m} R_{\tilde{b}\tilde{b}N}^{n,l*} R_{\tilde{b}\tilde{b}N}^{n,m} \right) \\ &\quad \times f_{ffs}(M_Z^2; m_{N_m}, M_{\tilde{b}_m}, m_{N_l}) \\ &+ \frac{e}{2s_W c_W} \sum_{n,m,l} \left(L_{ZNN}^{l,m} L_{\tilde{b}\tilde{b}N}^{n,l*} L_{\tilde{b}\tilde{b}N}^{n,m} + R_{ZNN}^{l,m} R_{\tilde{b}\tilde{b}N}^{n,l*} R_{\tilde{b}\tilde{b}N}^{n,m} \right) \\ &\quad \times m_{N_m} m_{N_l} c_0(M_Z^2; m_{N_m}, M_{\tilde{b}_m}, m_{N_l}) \end{aligned} \quad (45)$$

$$\begin{aligned} \delta F_A^{(N)} &= -\frac{e}{2s_W c_W} \sum_{n,m,l} \left(R_{ZNN}^{l,m} L_{\tilde{b}\tilde{b}N}^{n,l*} L_{\tilde{b}\tilde{b}N}^{n,m} - L_{ZNN}^{l,m} R_{\tilde{b}\tilde{b}N}^{n,l*} R_{\tilde{b}\tilde{b}N}^{n,m} \right) \\ &\quad \times f_{ffs}(M_Z^2; m_{N_m}, M_{\tilde{b}_m}, m_{N_l}) \\ &+ \frac{e}{2s_W c_W} \sum_{n,m,l} \left(L_{ZNN}^{l,m} L_{\tilde{b}\tilde{b}N}^{n,l*} L_{\tilde{b}\tilde{b}N}^{n,m} - R_{ZNN}^{l,m} R_{\tilde{b}\tilde{b}N}^{n,l*} R_{\tilde{b}\tilde{b}N}^{n,m} \right) \\ &\quad \times m_{N_m} m_{N_l} c_0(M_Z^2; m_{N_m}, M_{\tilde{b}_m}, m_{N_l}) \end{aligned} \quad (46)$$

where the couplings can be found in [20] and read:

$$\begin{aligned} L_{ZNN}^{l,m} &= Z_N^{4l*} Z_N^{4m} - Z_N^{3l*} Z_N^{3m} \\ R_{ZNN}^{l,m} &= Z_N^{3l} Z_N^{3m*} - Z_N^{4l} Z_N^{4m*} \end{aligned} \quad (47)$$

$$V_{Z\bar{b}\bar{b}}^{l,m} = B^{1l} B^{1m} - \frac{2}{3} s_W^2 \delta^{lm} \quad (48)$$

$$\begin{aligned} L_{\bar{b}\bar{b}N}^{n,l} &= \frac{e}{\sqrt{2} s_W c_W} \left[B^{1n} \left(\frac{1}{3} s_W Z_N^{1l} - c_W Z_N^{2l} \right) + \frac{m_b}{M_Z \cos \beta} B^{2n} Z_N^{3l} \right] \\ R_{\bar{b}\bar{b}N}^{n,l} &= \frac{\sqrt{2} e}{3 c_W} B^{2n} Z_N^{1l*} + \frac{e}{\sqrt{2} s_W c_W} \frac{m_b}{M_Z \cos \beta} B^{1n} Z_N^{3l*} \end{aligned} \quad (49)$$

where the matrix Z_N diagonalizes the neutralino mass matrix and the matrix B^{ij} for sbottom quarks is defined in the same way as the matrix T^{ij} for stops in eq. (20).

APPENDIX B.

Here we give expressions for the functions f_{ssf} and f_{fss} needed to compute SUSY contributions to the $Z^0\bar{b}b$ vertex.

$$\begin{aligned}
f_{ssf}(s, m_1, m_2, m_3) &= -\frac{1}{2} + \frac{1}{2s} (a_0(m_1) + a_0(m_3) - 2a_0(m_2)) \\
&+ \frac{s - m_1^2 - m_3^2 + 2m_2^2}{2s} b_0(s, m_1, m_3) \\
&+ \left(m_2^2 + \frac{(m_1^2 - m_2^2)(m_3^2 - m_2^2)}{s} \right) c_0(m_1, m_2, m_3) \\
&- \frac{1}{4} b_0(0, m_2, m_1) - \frac{1}{4} (m_2^2 - m_1^2) b'_0(m_2, m_1) \\
&- \frac{1}{4} b_0(0, m_2, m_3) - \frac{1}{4} (m_2^2 - m_3^2) b'_0(m_2, m_3)
\end{aligned} \tag{50}$$

$$\begin{aligned}
f_{ffs}(s; m_1, m_2, m_3) &= \frac{1}{2} + \frac{s + m_1^2 + m_3^2 - 2m_2^2}{2s} b_0(s, m_1, m_3) \\
&- \frac{1}{2s} (a_0(m_1) + a_0(m_3) - 2a_0(m_2)) \\
&- \frac{(m_1^2 - m_2^2)(m_3^2 - m_2^2)}{s} c_0(m_1, m_2, m_3) \\
&- \frac{1}{4} b_0(0, m_1, m_2) - \frac{1}{4} (m_1^2 - m_2^2) b'_0(m_1, m_2) \\
&- \frac{1}{4} b_0(0, m_3, m_2) - \frac{1}{4} (m_3^2 - m_2^2) b'_0(m_3, m_2)
\end{aligned} \tag{51}$$

Standard two-point functions used in eqs. (51,52) read:

$$a_0(m) = m^2 \left(\eta - 1 + \log \frac{m^2}{Q^2} \right) \tag{52}$$

$$b_0(s, m_1, m_2) = \eta + \int_0^1 dx \log \frac{x(x-1)s + xm_1^2 + (1-x)m_2^2}{Q^2} \tag{53}$$

Q^2 is the \overline{MS} renormalization scale and $\eta \equiv 2/(d-4)$. Derivative at $s=0$ of $b_0(s, m_1, m_2)$ reads:

$$b'_0(m_1, m_2) = -\frac{1}{2} \frac{m_1^2 + m_2^2}{(m_1^2 - m_2^2)^2} + \frac{m_1^2 m_2^2}{(m_1^2 - m_2^2)^3} \log \frac{m_1^2}{m_2^2} \tag{54}$$

Finally, the $c_0(m_1, m_2, m_3)$ function is defined as:

$$c_0(m_1, m_2, m_3) = \int \frac{d^4 k}{\pi^2} \frac{i}{[k^2 - m_1^2][(k+p)^2 - m_2^2][(k+p+q)^2 - m_3^2]} \tag{55}$$

In the case of the $Z^0\bar{b}b$ vertex $(p+q)^2 = M_Z^2$ and we $p^2 = q^2 = m_b^2 \approx 0$.

References

- [1] J.T. Liu, D. Ng *Phys. Lett.* **342B** (1994) 262,
D. Ng in Proceedings. of the Beyond the Standard Model IV conference, Lake Tahoe C.A., eds. J.F. Gunion, T. Han, J. Ohnemus (1994),
E. Ma, D. Ng preprint UCRHEP-T-144 (hep-ph/9505268),
J.K. Kim, Y.G. Kim, J.S. Lee, K.Y. Lee preprint KAIST-CHEP-95-14 (hep-ph/9509319),
E. Simmons, R.S. Chivukula, J. Terning preprint BU-HEP-95-27 (hep-ph/9509392),
E. Ma, preprint UCRHEP-T-153 (hep-ph/9510289),
G. Bhattacharyya, G. Branco, W.S. Hou preprint CERN-TH/95-326 (hep-ph/9512239),
T. Yoshikawa preprint HUPD-9528 (hep-ph/9512251),
Z.-J. Xiao, L.-D. Wan, G.-R. Lu, X.-L. Wang *J. Phys.* **G21** (1995) 167,
G. Altarelli et al. preprint CERN-TH/96-20 (hep-ph/9601324),
P. Chiappetta et al. preprint CPT-96/P.3304 (hep-ph/9601306).
- [2] G. Altarelli, R. Barbieri F. Caravaglios *Phys. Lett.* **314B** (1993) 357,
G.L. Kane C. Kolda J.D. Wells. *Phys. Lett.* **338B** (1994) 219,
P.H. Chankowski, S. Pokorski in Proceedings. of the Beyond the Standard Model IV conference, Lake Tahoe C.A., eds. J.F. Gunion, T. Han, J. Ohnemus (1994) p. 233,
D. Garcia, R. Jimenéz J. Solà *Phys. Lett.* **347** (1995) 309, 321, E **351B** (1995) 602,
D. Garcia, J. Solà *Phys. Lett.* **354B** (1995) 335, **357B** (1995) 349,
M. Carena, C. Wagner *Nucl. Phys.* **B452** (1995) 45,
X. Wang, J.L. Lopez, D.V. Nanopoulos preprint CERN-TH/95-7553 (hep-ph/9501258) and *Phys. Rev.* **D52** (1995) 4116,
A. Dabelstein, W. Hollik, W. Möhle preprint KA-THEP-5-1995 (hep-ph/9506251).
- [3] J. Erler, P. Langacker *Phys. Rev.* **D52** (1995) 441.
- [4] G.L. Kane R.G. Stuart, J.D. Wells *Phys. Lett.* **354B** (1995) 350.
- [5] see P.H. Chankowski, S. Pokorski in ref. [2] and *Phys. Lett.* **366B** (1996) 188.
- [6] P.H. Chankowski contribution to the International Europhysics Conference on High Energy Physics, Brussels, 27 July – 2 August, 1995, to appear in the Proceedings,
S. Pokorski “Status of the MSSM”, at SUSY’95 International Conference, Ecole Polytechnique, Palaiseau, May 1995, to appear in the Proceedings (hep-ph/9510224).

- [7] M. Shifman *Mod. Phys. Lett.* **A10** (1995) 605.
- [8] G.L. Kane, J.D. Wells preprint SLAC-PUB-95-7038 (1995) (hep-ph/9510372)
- [9] J. Ellis, J.L. Lopez, D.V. Nanopoulos preprint CERN-TH/95-314 (hep-ph/9512288).
- [10] The LEP Electroweak Working Group, CERN preprint CERN/PPE/94-187, LEPEWWG/95-01, LEPEWWG/95-02.
- [11] A. Olchevski, plenary talk at the International Europhysics Conference on High Energy Physics, Brussels, 27 July – 2 August, 1995,
D. Charlton, talk at the International Europhysics Conference on High Energy Physics, Brussels, 27 July – 2 August, 1995.
- [12] M. Boulware, D. Finnell *Phys. Rev.* **D44** (1991) 2054,
J. Rosiek *Phys. Lett.* **252B** (1990) 135,
A.Denner et al. *Z. Phys.* **C51** (1991) 695.
- [13] J. Ellis, G.L. Fogli, E. Lisi *Phys. Lett.* **292B** (1992) 427, **318B** (1993) 375, **324B** (1994) 173. **333B** (1994) 118,
G. Altarelli, R. Barbieri *Phys. Lett.* **253B** (1991) 161,
G. Altarelli, R. Barbieri, S. Jadach *Nucl. Phys.* **B369** (1992) 3,
J. Ellis, G.L. Fogli, E. Lisi preprint CERN-TH/95-202 (hep-ph/9507424).
- [14] P.H. Chankowski, S. Pokorski *Phys. Lett.* **356B** (1995) 307, and hep-ph/9509207 to appear in *Acta. Phys. Pol.* **B** (1996).
- [15] M. Virchaux and A. Milsztajn, *Phys. Lett.* **274B** (1992) 221.
- [16] C. Michael talk given at International Symposium on Lepton Photon Interactions (IHEP), Beijing, P.R. China, August 1995, to be published in the Proceedings, preprint LTH-358, (hep-ph/9510203).
- [17] G. Altarelli in Proc. of the 1992 Aachen Workshop, eds P. Zerwas and H. Kastrup, World Scientific, Singapore 1993, vol.1 p. 172,
see also S. Bethke talk at Rencontres de Moriond, March 1995.
- [18] G.F. Giudice, M.L. Mangano et al. (hep-ph/9602207)
- [19] P.H. Chankowski et al. *Nucl. Phys.* **B417** (1994), 101.
- [20] J. Rosiek *Phys. Rev.* **D41** (1990) 3464, preprint KA-TP-8-1995 (hep-ph/9511250).

- [21] C. Quigg preprint FERMILAB-CONF-95/139-T,
J. Incandela preprint FERMILAB-CONF-95/162-E.
- [22] S. Mrenna, C.-P. Yuan preprint ANL-HEP-PR-95-66 (1995) (hep-ph/9509424).
- [23] S. Abachi et al. (D0 Collaboration) preprint FERMILAB-PUB-95-380-E (1995).
- [24] L. Rolandi, H. Dijkstra, D. Strickland and G. Wilson (ALEPH, DELPHI, L3 and OPAL collaborations), Joint Seminar on the First Results from LEP1.5, CERN, Dec. 1995.
- [25] R. Hempfling Ph.D. Thesis, UCSC preprint SCIPP 92/28 (1992),
J.L. Lopez, D.V. Nanopoulos *Phys. Lett.* **266B** (1991) 397.
- [26] A. Ali, C. Greub *Phys. Lett.* **293B** (1992) 226,
A. Buras, M. Misiak, M. Münz, S. Pokorski *Nucl. Phys.* **B424** (1994) 376.
- [27] R. Barbieri, G.F. Giudice *Phys. Lett.* **309B** (1993) 86.
- [28] A. Blondel, C. Verzegnassi *Phys. Lett.* **311B** (1993) 346.
- [29] A. Brignole, F. Feruglio, F. Zwirner preprint CERN-TH-95-340 (hep-ph/9601293).
- [30] R. Barbieri, F. Caravaglios, M. Frigeni *Phys. Lett.* **279B** (1992) 169.
- [31] J. Ellis, G. Ridolfi, F. Zwirner *Phys. Lett.* **262B** (1991) 477.
- [32] P. Krawczyk, S. Pokorski *Phys. Rev. Lett.* **60** (1988) 182,
G. Isidori *Phys. Lett.* **298B** (1993) 409,
Y. Grossman, H.E. Haber, Y. Nir preprint CERN-TH/95-182 (hep-ph/9507213).
- [33] The ALEPH Collaboration contribution to the International Europhysics Conference on High Energy Physics, Brussels, 27 July – 2 August, 1995, paper EPS0415.

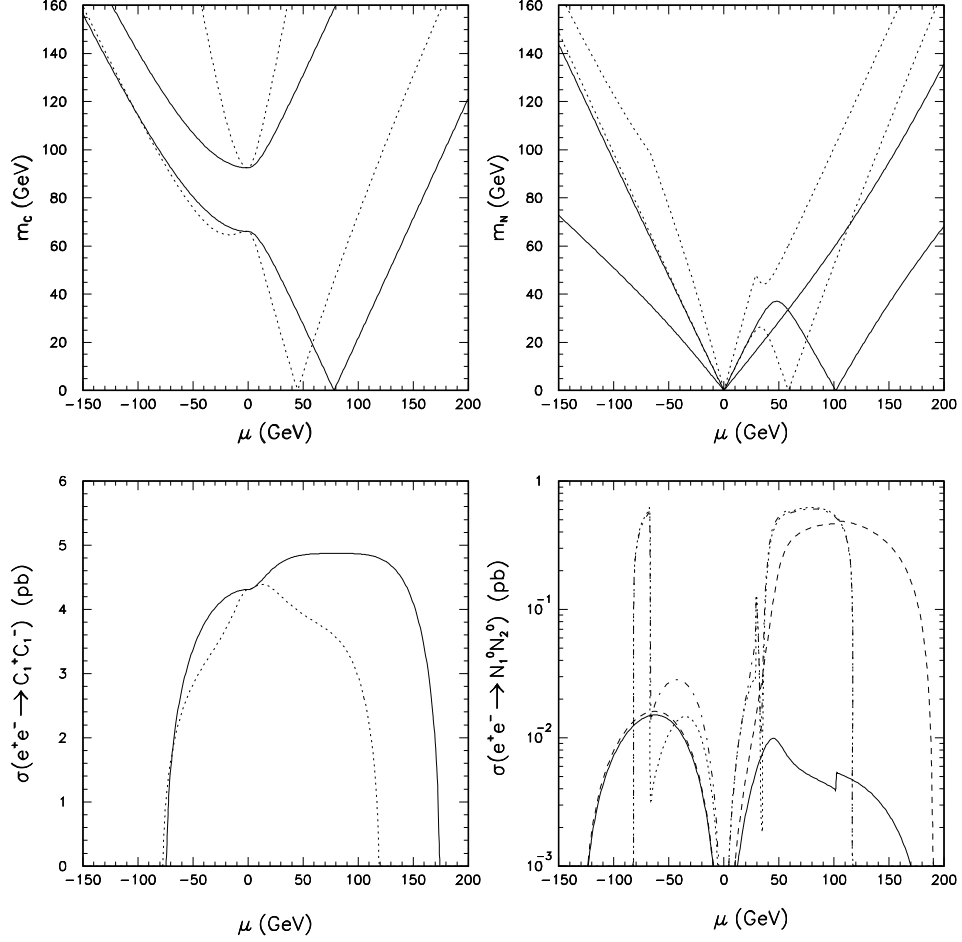


Figure 1: Masses of the two charginos and two lightest neutralinos as a function of μ for $r = 1$ (solid lines) and $r = 3$ (dotted lines) for $\tan\beta = 1.4$. In the lower panels the corresponding production cross sections of $C_1^+ C_1^-$ and $N_1^0 N_2^0$ at LEP2 ($s^{1/2} = 190$ GeV) are shown. Masses of the sparticles exchanged in the t channel are taken to be $M_{\tilde{\nu}_e} = M_{\tilde{e}_R} = 500$ GeV. For neutralinos also the case $M_{\tilde{e}_R} = 50$ GeV (dashed and dash-dotted lines for $r = 1$ and $r = 3$ respectively) is shown.

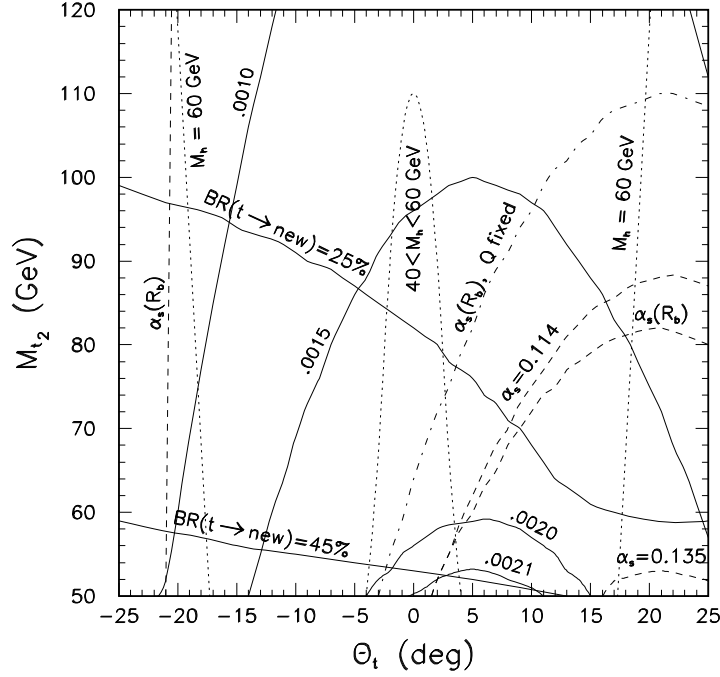


Figure 2: Contours of constant δR_b^{SU5Y} (solid lines) and various constraints in the plane (θ_t, M_{t_2}) for $m_t = 170$ GeV, $\tan\beta = 1.4$, $M_2 = -\mu = 58$ GeV ($m_{C_1} = 85$ GeV), $M_A = M_{\tilde{t}_1} = 1$ TeV. Dashed and dash-dotted lines show the $b \rightarrow s\gamma$ constraint with different treatment of α_s : $\alpha_s(R_b)$ denotes the curves obtained with $\alpha_s(M_Z) = 0.123 - 4\delta R_b^{SU5Y}$ and with the renormalization scale Q varied in the range $(m_b/2, 2m_b)$. The curve with Q fixed correspond to $Q = m_b = 4.7$ GeV and $\alpha_s(M_Z) = 0.123$ (for more details see the text). Dotted lines illustrate the Higgs boson mass constraint. The allowed region is bounded from below by the $BR(t \rightarrow new) = 45\%$ curve and the parabolic $b \rightarrow s\gamma$ curve $\alpha_s(R_b)$ and from the left- and right- hand sides by the dotted curves $M_h = 60$ GeV. The area below the central dotted curve is also excluded.

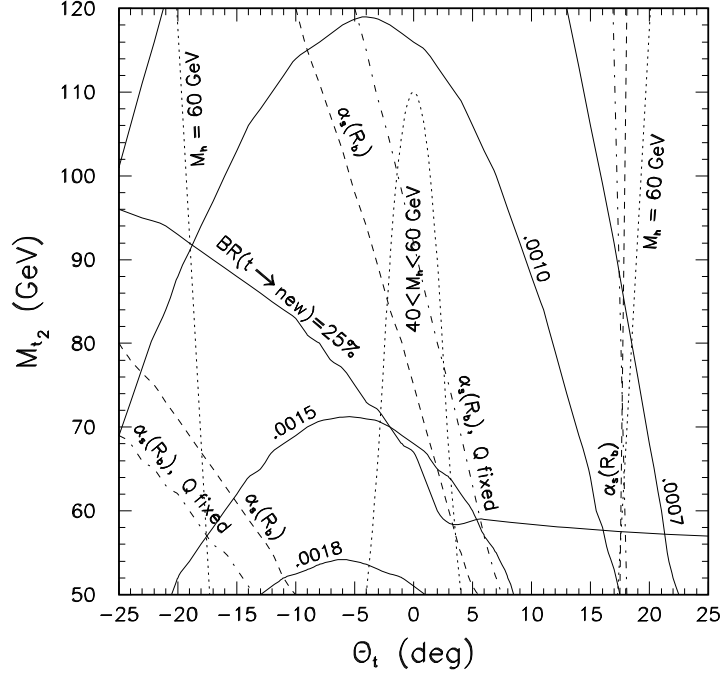


Figure 3: As in Fig. 2 but for $\mu > 0$ and $r = 1.5$. $\mu = 85.5$ GeV ($m_{C_1} = 55$ GeV), $M_A = M_{\tilde{t}_1} = 1$ TeV. The allowed region is for $\theta_t > 0$, between the two dashed curves denoted by $\alpha_s(R_b)$ (with exclusion of the central area $40 < M_h < 60$ GeV) and for $\theta_t < 0$, below the dashed curve $\alpha_s(R_b)$ (bounded from the left by the dotted curve $M_h = 60$ GeV).

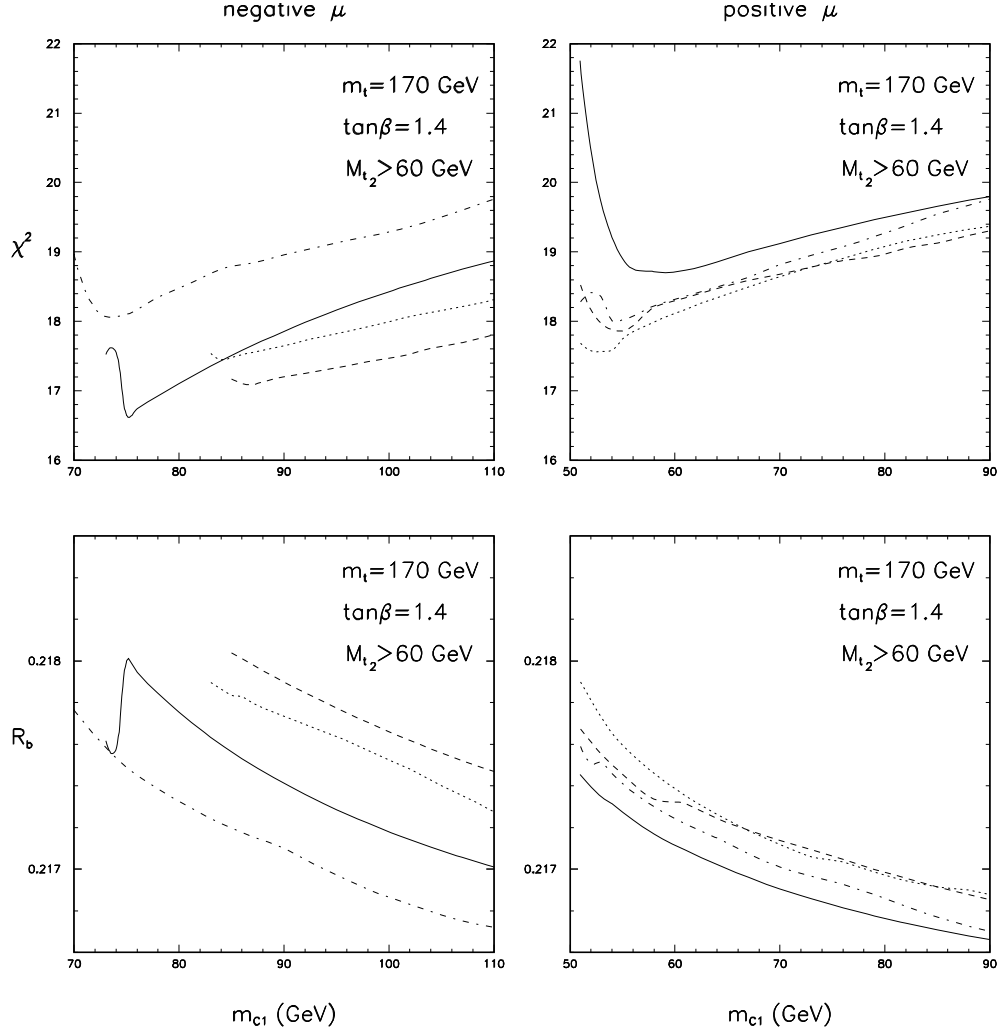


Figure 4: χ^2 as a function of m_{C_1} for $r \equiv M_2/|\mu| = 0.5$ (solid lines), 1 (dashed), 1.5 (dotted), and 3 (dash-dotted) for both signs of μ for $m_t = 170$ GeV, $\tan\beta = 1.4$, $M_A = M_{\tilde{t}_1} = 1$ TeV. In lower pannels the best values of R_b with the restriction $\chi^2 < \chi_{min}^2 + 1$ (here χ_{min}^2 denotes the best χ^2 for fixed value of m_{C_1}) are shown. In addition we required $M_{\tilde{t}_2} > 60$ GeV.

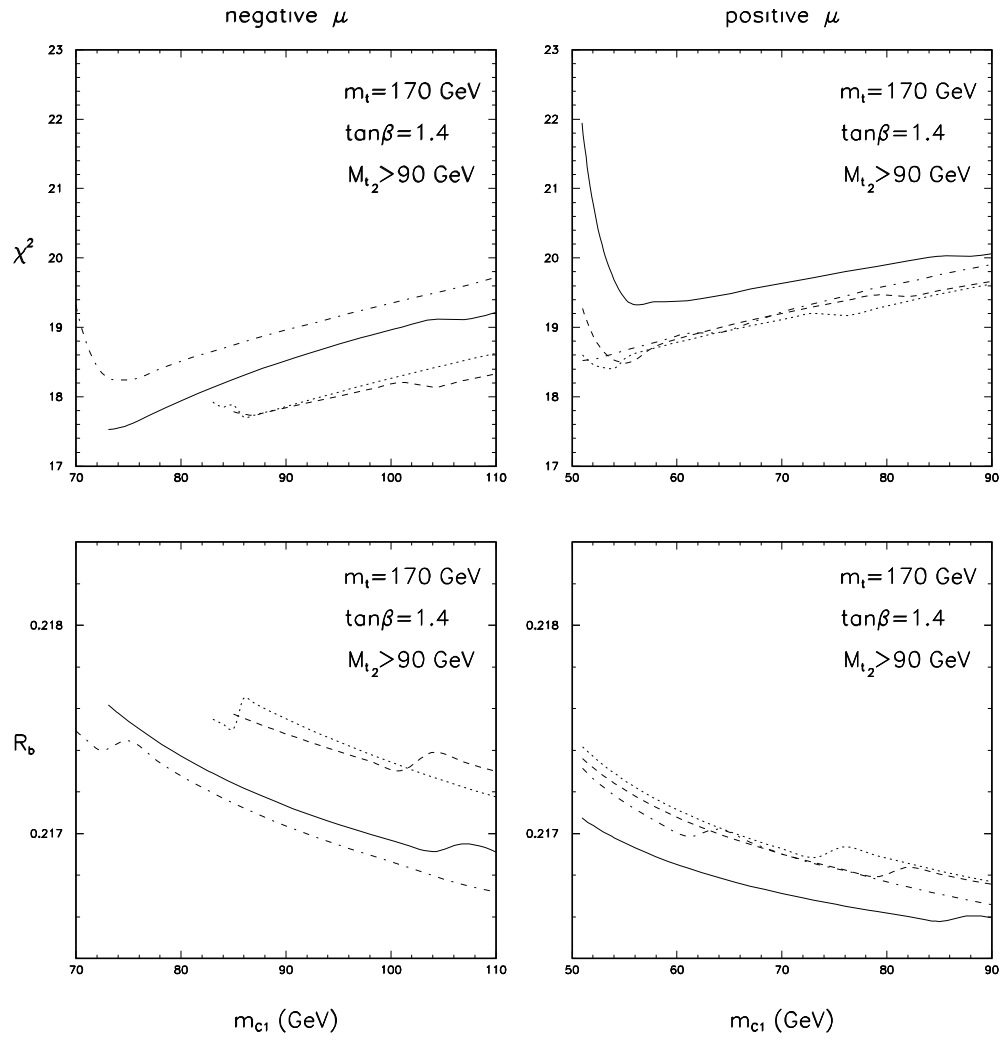


Figure 5: As in Fig. 4 but with condition $M_{\tilde{t}_2} > 90$ GeV.

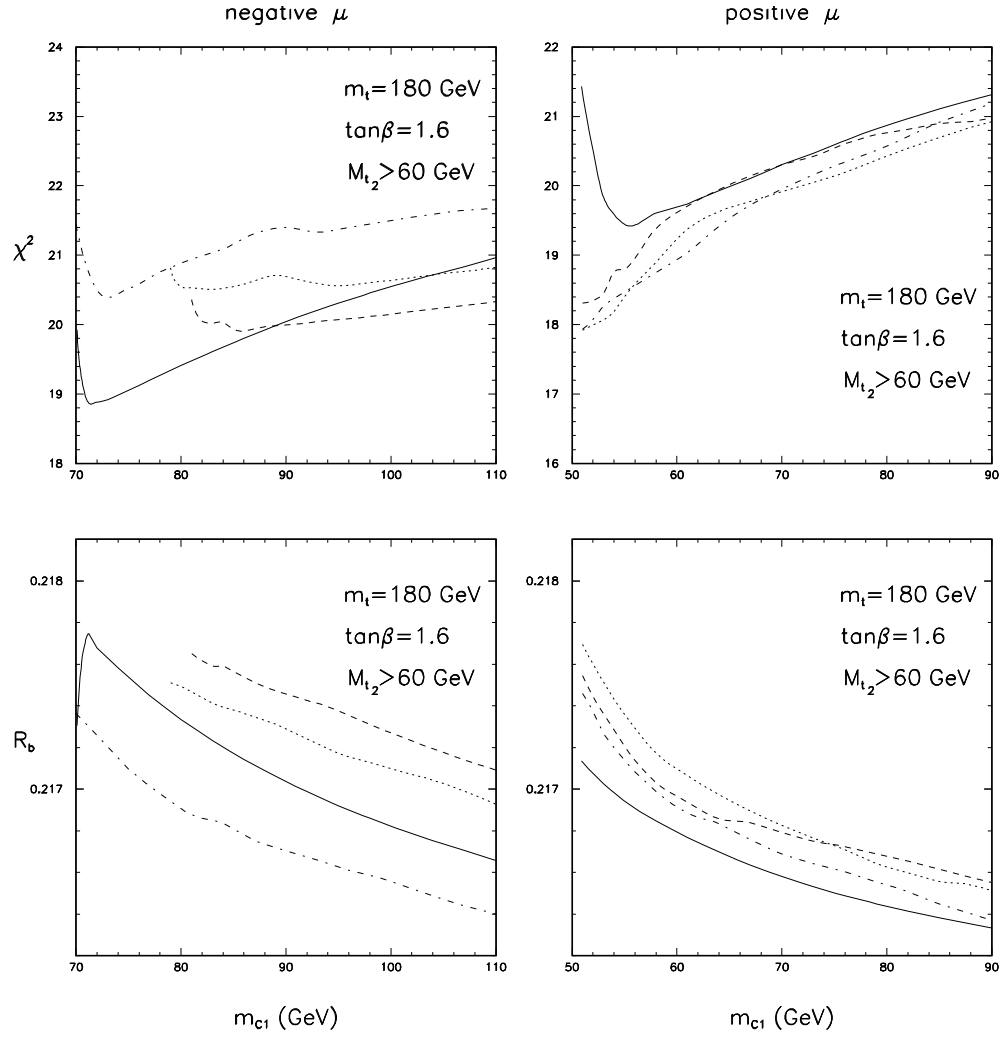


Figure 6: As in Fig. 4 but for $m_t = 180$.

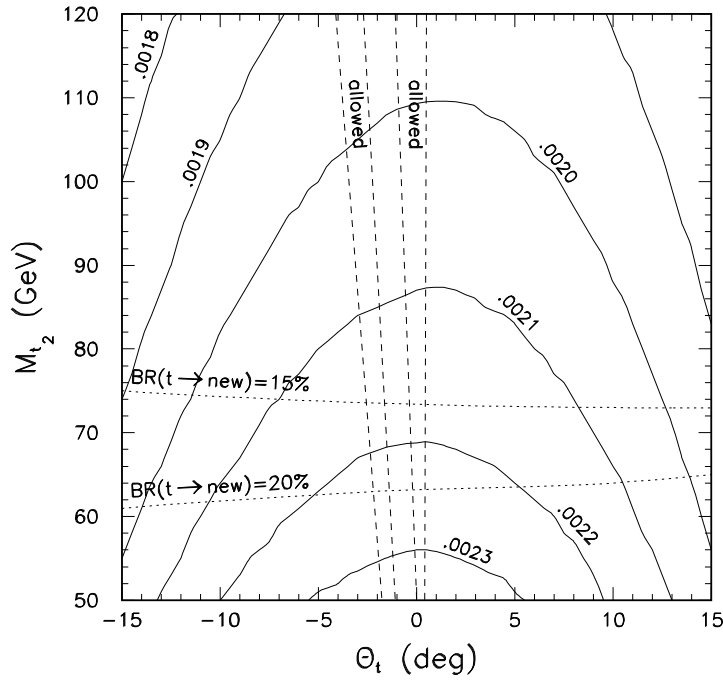


Figure 7: Contours of constant δR_b^{SUSY} (solid lines) and allowed by $BR(b \rightarrow s\gamma)$ regions in the $(\theta_t, M_{\tilde{t}_2})$ plane for $m_t = 170$ GeV, $\tan\beta = 50$, $M_2 = 1.5\mu$, $m_{C_1} = 65$ GeV, $M_{\tilde{t}_1} = 1$ TeV, $M_A = 55$ GeV and $M_{\tilde{b}_R} = 130$ GeV. Contours of constant $\sum_i BR(t \rightarrow \tilde{t}_2 N_i^0)$ are also shown (dotted lines).

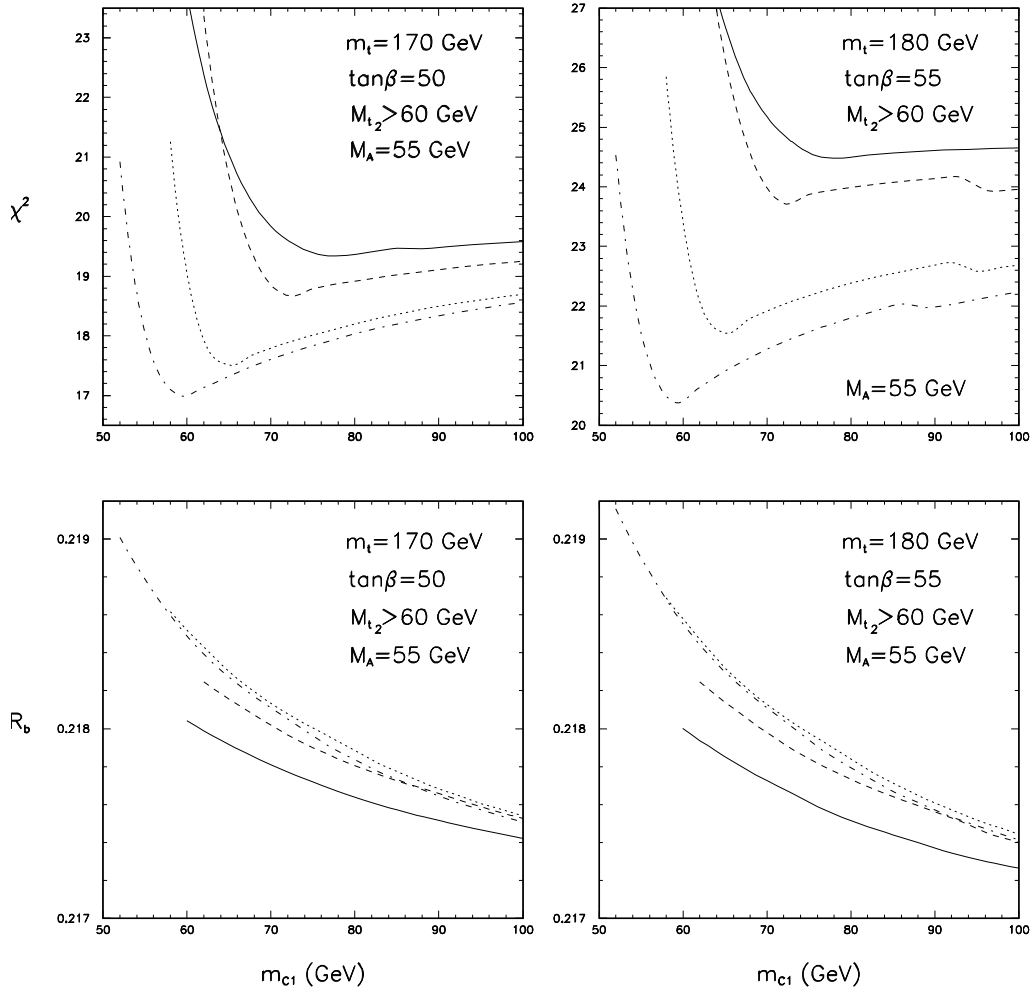


Figure 8: χ^2 as a function of m_{C_1} ($\mu > 0$) for $r \equiv M_2/|\mu| = 1$ (solid lines), 1.5 (dashed), 3 (dotted), and 5 (dash-dotted) for $m_t = 170$ GeV, $\tan\beta = 50$ and 180 GeV, $\tan\beta = 55$. $M_{\tilde{t}_1} = 1$ TeV, $M_A = 55$ GeV, $M_{\tilde{b}_R} = 130$ GeV. In lower panels the best values of R_b with the restriction $\chi^2 < \chi_{min}^2 + 1$ (here χ_{min}^2 denotes the best χ^2 for fixed value of m_{C_1}) are shown. In addition we required $M_{\tilde{t}_2} > 60$ GeV.

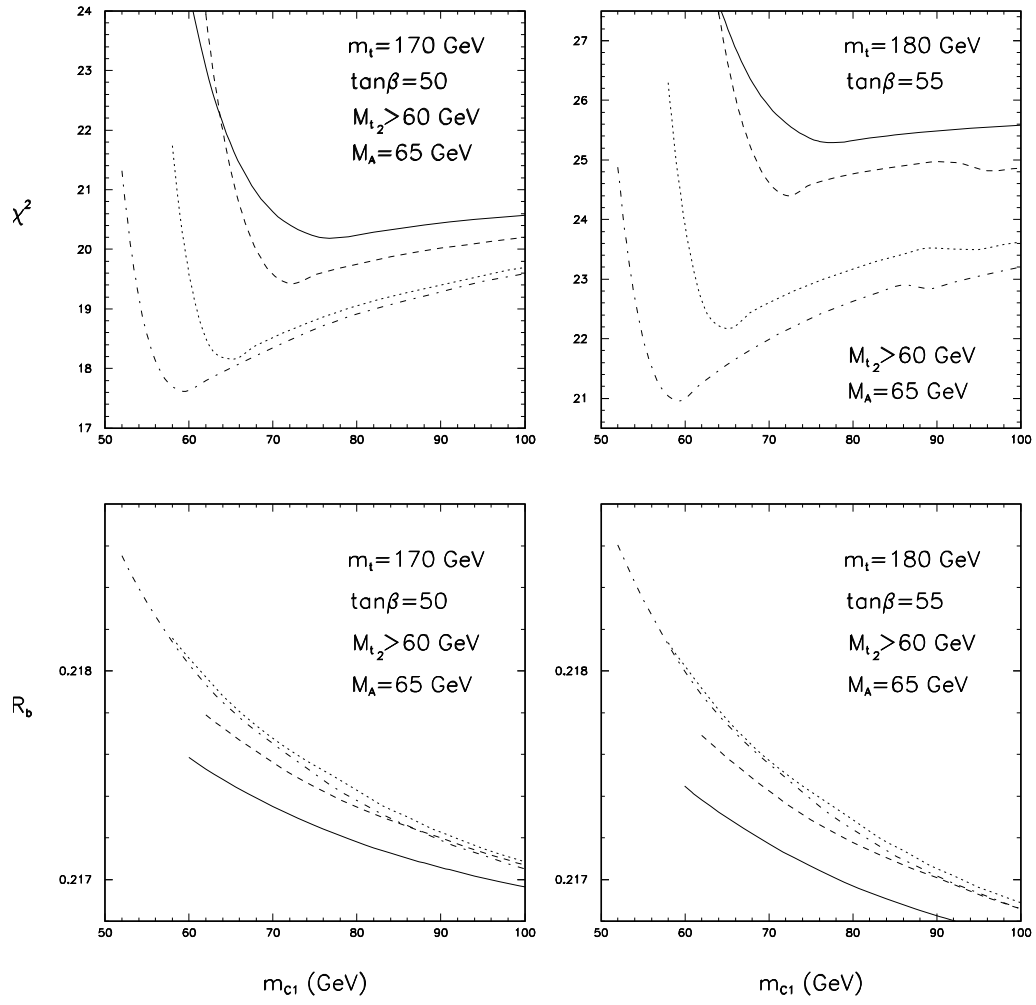


Figure 9: As in Fig. 8 but for $M_A = 65$ GeV.